Supplementary Analytical Techniques and results

S1 LASER FLUORINATION WHOLE ROCK OXYGEN ISOTOPE ANALYSES

Whole rock laser fluorination analysis was conducted at the University of Wisconsin, Madison following the techniques of Valley et al. (1995). The UWG-2 garnet standard was analyzed a total of 6 times before and after the dyke WR powders. The garnet standard results were very reproducible giving a raw oxygen isotopic composition of 5.70 ± 0.12 ‰ 2σ, which is within the accepted range for the standard ($\delta^{18}O$ = 5.8‰ VSMOW, Valley et al. 1995).

S2 IMAGING

CL and backscattered electron (BSE) imaging was conducted on all zircons prior to analysis to document internal structures of the grains. Imaging was conducted at CCIM using a Zeiss EVO 15 scanning electron microscope equipped with a Robinson wide spectrum CL detector, secondary electron and backscattered electron detector. Typical beam conditions were 15 kV and 3 – 5 nA.

S3 LASER ABLATION MULTI COLLECTOR INDUCTIVELY COUPLED PLASMA MASS SPECTROMETRY (LA-MC-ICP-MS)

U-Pb geochronology of zircons from NAPI and JD09-2 was conducted at the Radiogenic Isotope Facility (RIF) at the University of Alberta. A detailed description of the analytical techniques is provided by Simonetti et al. (2005), so only an overview is provided here. Data were collected using a Nu Plasma I MC-ICP-MS coupled to a New Wave Research™ UP 213 Nd:YAG laser ablation system operating with a wavelength of 213 nm. We ablated the zircons using a 30 μm diameter laser beam with an energy density of 2-3 J/cm^2 and a repetition rate of 4 Hz. The vaporized material was simultaneously mixed with a Tl solution using a desolvating nebulization system and transported in a He carrier gas to the torch of the MC-ICP-MS where all of the material was ionized in an Ar plasma. A total analytical sequence consisted of a 4 second laser warm up, a pre-ablation pass plus 3 second magnet settling time, and 30*1 second integrations of data collection plus additional delays between each integration for a total duty cycle of approximately 70 seconds. Between each analysis we allowed 15-20 seconds of washout to clear the laser cell. Lead isotope ratios were corrected for mass bias using an exponential law and assuming a $^{205}Tl/^{203}Tl$ of 2.3871, while U-Pb fractionation and instrument drift was accounted for using a sample standard bracketing technique. An in-house zircon standard (LH94-15, Ashton et al. 1999) was analyzed 3 times ten

unknowns along with a secondary standard (OG1-1, Stern et al. 2009) to assess data quality. The average $^{207}Pb/^{206}Pb$ of LH94-15 over the analytical period was 0.11193 ± 0.00092 2σ (n=10 MSWD = 23) which is in excellent agreement with the published ID-TIMS value of 0.11187 ± 0.00004 (Ashton et al. 1999). OG1 produced a weighted average $^{207}Pb/^{206}Pb$ age of 3458.0 ± 7.1 Ma (n= 6, MSWD = 0.1) which is a slightly younger, but within error of the published TIMS and SIMS age for this standard of 3465.4 ± 0.6 Ma (Stern et al. 2009; Table 1). The $^{204}(Hg+Pb)$ acid+gas blank was found to be consistent before and after ablation, which enabled the effects of ^{204}Pb background and ^{204}Hg interference to be subtracted from each analysis. Any excess on mass 204 after blank subtraction is attributed to a common Pb component within the zircon crystal. Samples NAPI and OG1 both had low ^{204}Pb counts, however, JD09-2 contained more ^{204}Pb (100-1000 cps ^{204}Pb). High $^{206}Pb/^{204}Pb$ values for JD09-2 (>1000) indicate that the common Pb component was minor relative to the radiogenic Pb, and so no common Pb correction was performed. Despite the high ^{204}Pb in JD09-2, the main source of uncertainty for this analysis is the external reproducibility which is estimated at ~2.5 % for U/Pb and ~1 % for $^{207}Pb/^{206}Pb$ in this analytical session.

S4 RAMAN BAND FITTING

The line width (full width at half maximum - FWHM) and the frequency (peak center) of the asymmetrical $\nu_3(SiO_4)$ stretching band was used to determine the degree of metamictization within the zircons (Nasdala et al. 1995), and also to determine the age of α-dose retention (e.g. Nasdala et al. 2001; 2004). Estimating the band parameters accurately and quantifying the uncertainty in the fit is essential to interpreting Raman spectra, and comparing results between studies. Raman bands in minerals are often nonsymmetrical in profile due to interferences between bands. In the case of metamict zircon, the $\nu_3(SiO_4)$ band is overlapped by the $\nu_1(SiO_4)$ band, making extraction of the peak parameters for the $\nu_3(SiO_4)$ band more difficult. To obtain the relevant parameters of the $\nu_3(SiO_4)$ band (linewidth and peak center), the contribution from the $\nu_1(SiO_4)$ stretching mode at ~975 cm^{-1} (A_{1g} symmetry; Dawson et al. 1971) and the broad band associated with the amorphous component of metamict zircon (Geisler et al. 2001; Zhang et al. 2000) need to be subtracted.

When fitting a model to the data there are numerous parameters to consider, e.g. the type of model (Gaussian, Lorentzian etc.); the number of functions; the goodness of fit (chi square, reduced chi square, etc.). The type of model used to fit the data officially implies a physical characteristic of the phonon frequency that is being modeled. For example, phonons produced in a perfectly crystalline material have a long lifetime and their

peak can be perfectly modeled by a Lorentzian function. As disorder is introduced to the crystal structure (though elemental substitutions, metamictization, Frenkel defects etc.), phonons have a shorter lifetime and the subsequent phonon peak becomes broader. Broader peaks may be modeled more accurately with a Gaussian or Voigt function, both of which can account for the disorder in the crystal. The samples in this study represent a continuum from crystalline material to metamict, we therefore analyzed all of the data using Lorentzian, Voigt and Gaussian functions and chose the model which best fits the data. Also, because of the large number of Raman spectra to analyze (>100) we developed an automated procedure for fitting the data, the details of the procedure are described below.

The region of interest in the Raman spectra is between 850 and 1150 cm^{-1} containing both ν_1 (SiO$_4$) and ν_3 (SiO$_4$) modes. Before any fitting, the Raman background is subtracted, but since there is no simple model to fit the background, we use a third order polynomial function to fit the spectra in the region preceding and following the phonon peaks, therefore only removing the background (and the amorphous component) of the Raman spectra over the region of interest. After background subtraction we fit the ν_1 (SiO$_4$) and ν_3 (SiO$_4$) modes with two different peaks.

In order to assess the accuracy of the different fitting functions, we calculated a reduced chi squared statistic (χ^2/ν) for each fit, where $\nu = n-p-1$, n is the number of observations and p is the number of fitting parameters. The reduced chi squared statistic assesses the goodness of fit, and produces a value of 1 if the measurement error is perfectly accounted for by the model, values greater than or less than one indicate that the measurement error is too small or two large, respectively.

All of the models fit the peak center of the ν_3 (SiO$_4$) band relatively well (Fig. S1a) with the Voigt and Gaussian models differing from the Lorentzian model occasionally, although in general all three models agree in most of the samples. The FWHM (Fig. S1b) for the ν_3 (SiO$_4$) bands are more divergent between the models, with the Gaussian frequently producing a different result to the Voigt and Lorentzian. The Voigt model combines the Gaussian and Lorentzian functions and Fig. S1b indicates that the Voigt model preferentially takes the Lorentzian form most of the time, even in highly metamict samples.

The low reduced chi squared statistic indicates that all of the models fit the data well when the degree of metamictization is high (i.e. low wavenumbers for the peak center) (Fig. S1c). The accuracy of the fit at low wavenumbers is expected - as the peak becomes broader, more data points define the peak and it is easier for the model to fit. As the wavenumber for the ν_3 (SiO$_4$) band increases, the Gaussian models diverge significantly from the Raman spectra. The Gaussian model is expected to fail at high degrees of crystallinity (high wavenumbers) because phonons in crystalline materials show homogeneous broadening (where the interdeterminacy of the phonons under consideration is the same) and produce a Lorentzian profile. The Lorentzian and Voigt models fit the data equally well, although at higher degrees of crystallinity, the functions have difficulty resolving the apex of a very intense peak, and also struggle with the slight asymmetry of the shoulders of the ν_3 (SiO$_4$) band.
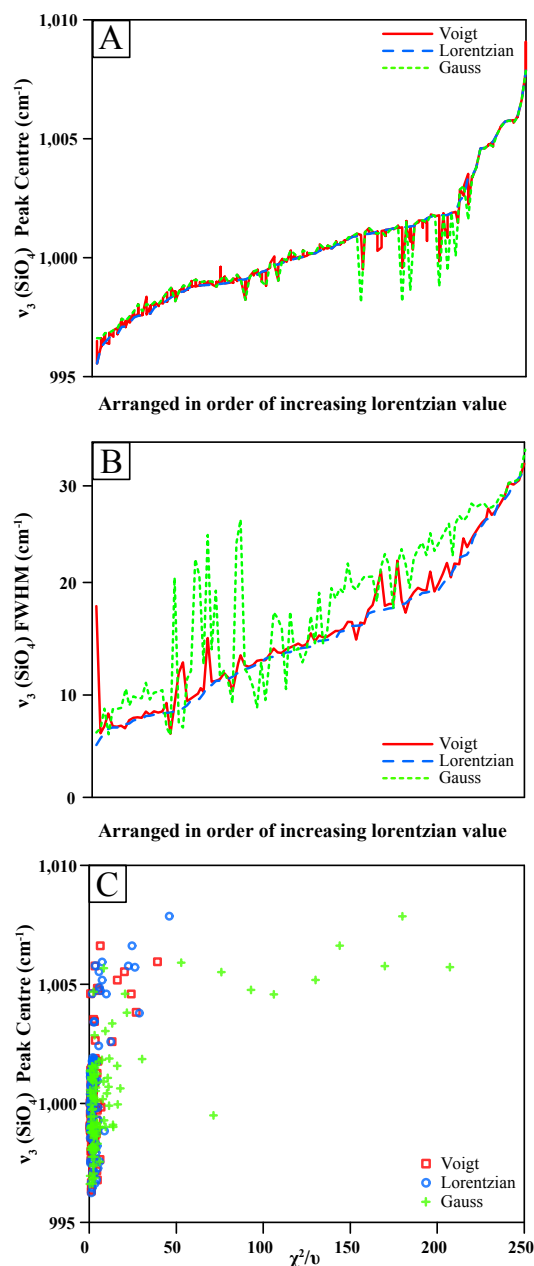
Supplementary Figure S1. Different numerical models for fitting the Raman spectra. A) peak centre for the ν3 (SiO4) band plotted for all of the samples using each model, the data are in order of increasing peak centre produced by the Lorentzian model. B) FWHM for the ν3 (SiO4) band plotted in the same way as A) in order of increasing Lorentzian value. C) reduced Chi squared statistic ($\chi 2/\nu$) plotted vs peak centre showing that peaks with high wavenumbers are most difficult for the Gaussian and Voigt distributions to model accurately. The Lorentzian model fits the data the best, accurately modeling the position of the ν1 (SiO4) and ν3 (SiO4) bands whereas the Gaussian and Voigt models produce low wavenumbers for the peak centre, and also overestimate the FWHM (see A and B as well).
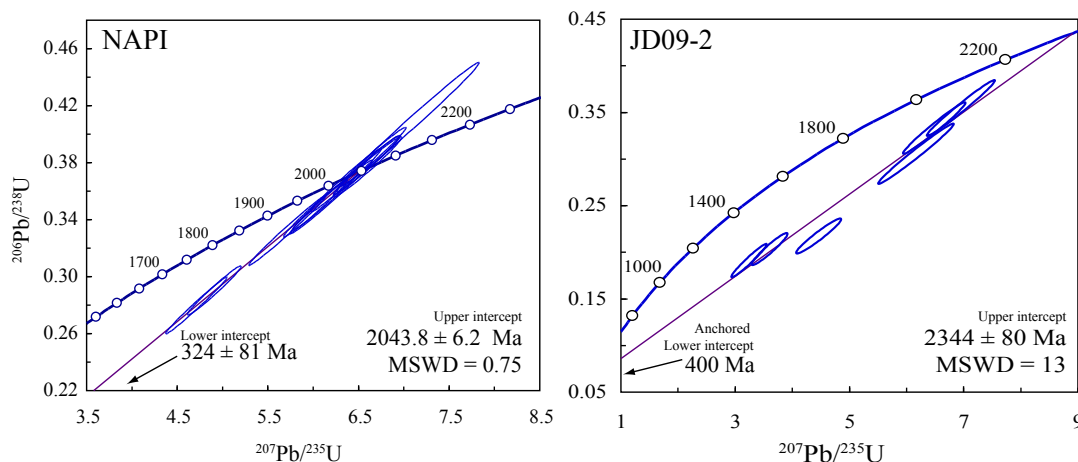
SUPPLEMENTARY FIGURE S2. Concordia diagrams of the LA-ICP-MS U-Pb data from the NAPI and JD09-2 samples. The ages are upper and lower intercept ages with 2σ errors. The error elipses are also at 2σ.

S5 U-Pb RESULTS

LA-MC-ICP-MS U-Pb zircon ages produced in this study are from the NAPI and JD09-2 dykes (Table 1, Fig. 3). The NAPI U-Pb zircon results are concordant or close to concordant with all analyses plotting along a discordia line with an upper intercept of 2043.8 ± 6.2 Ma and a lower intercept of 324 ± 81 Ma. The upper intercept age is not in agreement with the ~2400 Ma ages for other dykes in the Lewisian Gneiss Complex (Heaman and Tarney, 1989; Davies and Heaman, 2014), however the age is relatively close to a U-Pb baddeleyite age of 1992 +3/-2 Ma for an olivine gabbro dyke in the area (Heaman and Tarney, 1989). The lower intercept of 324 ± 81 Ma is in agreement with a Caledonian Pb-loss event, which was shown to have affected most zircons isolated from Scourie dykes (Davies and Heaman 2014).

The U-Pb zircon results from the JD09-2 dyke are much more complex. These zircons are all discordant (up to 50 %) with high common Pb contents (up to 2000 cps). The data broadly define a linear array with an upper intercept of 2344 ± 80 Ma with an anchored lower intercept at 400 Ma. Without the anchored lower intercept the crystallization age (upper intercept) stays the same, however the error increases by a factor of 10. The high common Pb for the JD09-2 zircons, and the uncertainty on the composition of this common Pb, mean that producing an accurate crystallization age is difficult. A general agreement with the ~2400 Ma ages from other dykes (Heaman and Tarney, 1989; Davies and Heaman, 2014) suggests that the JD09-2 zircons likely formed around this time, and similar to other zircon populations from Scourie dykes, may have experienced a Caledonian Pb-loss event.

In summary, both the dykes dated here, and the dykes dated previously (Heaman and Tarney, 1989; Davies and Heaman, 2014), produce ages in three broad categories: ~2.5 Ga from xenocrystic zircon and dyke emplacement ages of ~2.4 Ga and ~2.0 Ga. All the dykes were affected by a Pb-loss event during the Caledonian at ~400 Ma.

REFERENCES CITED

Ashton, K.E., Heaman, L.M., Lewry, J.F., Hartlaub, R.P., Shi, R., 1999. Age and origin of the Jan Lake Complex: a glimpse at the buried Archean craton of the Trans-Hudson Orogen. Canadian Journal of Earth Sciences 36, 185–208.

Davies, J.H.F.L., Heaman, L.M. 2014. New U-Pb baddeleyite and zircon ages for the Scourie dyke swarm: A long-lived large igneous province with implications for the Paleoproterozoic evolution of NW Scotland. Precambrian Research 249, 180-198.

Dawson, P., Hargreave, M.M., Wilkinson, G.R., 1971. The vibrational spectrum of zircon (ZrSiO₄). Journal of Physics C: Solid State Physics 4, 240-256.

Geisler, T., Pidgeon, R.T., van Bronswijk, W., Pleysier, R., 2001. Kinetics of thermal recovery and recrystallization of partially metamict zircon: a Raman spectroscopic study. European Journal of Mineralogy 13, 1163–1176. doi:10.1127/0935-1221/2001/0013-1163.

Heaman, L.M., Tarney, J., 1989. U-Pb baddeleyite ages for the Scourie dyke swarm, Scotland: evidence for two distinct intrusion events. Nature 340, 705–708.

Nasdala, L., Irmer, G., Wolf, D., 1995. The degree of metamictization in zircons: a Raman spectroscopic study. European Journal of Mineralogy 7, 471–478.

Nasdala, L., Wenzel, M., Vavra, G., Irmer, G., Wenzel, T., Kober, B., 2001. Metamictisation of natural zircon: accumulation versus thermal annealing of radioactivity-induced damage. Contributions to Mineralogy and Petrology 141, 125–144. doi:10.1007/s004100000235.

Nasdala, L., Reiners, P.W., Garver, J.I., Kennedy, A.K., Stern, R.A., Balan, E., Wirth, R., 2004. Incomplete retention of radiation damage in zircon from Sri Lanka. American Mineralogist 89: 219–231.

Simonetti, A., Heaman, L.M., Hartlaub, R.P., Creaser, R.A., MacHattie, T.G., Böhm, C., 2005. U–Pb zircon dating by laser ablation-MC-ICP-MS using a new multiple ion counting Faraday collector array. Journal of Analytical Atomic Spectrometry 20, 677–686. doi:10.1039/b504465k.

Stern, R.A., Bodorkos, S., Kamo, S.L., Hickman, A.H., Corfu, F., 2009. Measurement of SIMS instrumental mass fractionation of Pb isotopes during zircon dating. Geostandards and Geoanalytical Research 33, 145–168.

Valley, J.W., Kitchen, N., Kohn, M.J., Niendorf, C.R., Spicuzza, M.J., 1995. UWG-2, a garnet standard for oxygen isotope ratios: Strategies for high precision and accuracy with laser heating. Geochimich et Cosmochimica Acta 59, 5223-5231.

Zhang, M., Salje, E.K.H., Farnan, I., Graeme-Barber, A., Daniel, P., Ewing, R.C., Clark, A.M., Leroux, Hugues., 2000. Metamictization of zircon: Raman spectroscopic study. Journal of Physics: Condensed Matter 12, 1915-1925.